Icarus 211 (2011) 909–912

Contents lists available at ScienceDirect

Icarus

journal homepage: www.elsevier.com/locate/icarus

Note

Estimates of gravity wave drag on Mars: Indication of a possible lower thermospheric wind reversal

Alexander S. Medvedev [a,*], Erdal Yiğit [b], Paul Hartogh [a]

[a] Max Planck Institute for Solar System Research, Katlenburg-Lindau D-37191, Germany
[b] Center for Space Environment Modeling, Department of Atmosphere, Oceanic and Space Sciences, University of Michigan, Ann Arbor, MI 48109-2143, United States

ARTICLE INFO

Article history:
Received 27 July 2010
Revised 15 September 2010
Accepted 19 October 2010
Available online 30 October 2010

Keywords:
Atmospheres
Dynamics
Mars
Atmosphere

ABSTRACT

Spectral gravity wave parameterization suitable for planetary thermospheres applied to wind and temperature from Mars Climate Database reveals enormously strong drag incompatible with the wind distribution. It points out to a possible wind reversal in the 110–140 km layer similar to the one in the Earth's lower thermosphere.

1. Introduction

Gravity waves (GWs) are an intrinsic feature of all stably stratified planetary atmospheres. They play an important role in the vertical coupling by transporting momentum and energy between atmospheric layers. Large-scale circulation and temperature in the mesosphere and lower thermosphere (MLT) of Earth are strongly affected by GWs of lower atmospheric origin. Less is known about GWs and their significance on Mars, although observations suggest that disturbances attributed to GWs have amplitudes several times larger than on Earth in both the martian lower and upper atmospheres (Creasey et al., 2006a,b; Fritts et al., 2006). This results from a stronger than on Earth wave generation by wind shears and instabilities in lower atmospheric weather systems, volatile convection, and flow over the rugged topography.

Currently, there are very few observational estimates of possible dynamical effects of GWs in the upper atmosphere of Mars. Based on aerobraking density measurements from Mars Global Surveyor (MGS) and Mars Odyssey (ODY), Fritts et al. (2006) inferred that GW momentum deposition is of the order of 1000 m s^{-1} sol^{-1} at around 100 km. Recently, Heavens et al. (2010) found a possible GW saturation signal in convective instability or near-instability of temperature profiles retrieved from Mars Climate Sounder on Mars Reconnaissance Orbiter. They estimated that GW "drag" can reach up to 4500 m s^{-1} sol^{-1} at 0.1 Pa level (~80 km). These values are at least one order of magnitude larger than those in the terrestrial MLT.

More estimates of GW momentum flux divergences in the martian middle atmosphere (MA, 60–120 km) have been obtained in theoretical and modeling studies (Barnes, 1990; Théodore et al., 1993; Joshi et al., 1995; Collins et al., 1997). They had several features in common: (1) the upper boundaries of model domains were limited to ~80–100 km; (2) only terrain-generated harmonics with the observed phase velocity $c = 0$ were considered (except Théodore et al. (1993) who included also harmonics with $c = \pm 20$ m s^{-1}); (3) they all utilized the Lindzen parameterization for calculating the drag produced by individual subgrid-scale harmonics (with horizontal wavelengths 100–300 km). These studies demonstrated that the main influence of GWs is in the winter hemisphere near the edge of the westerly jet, magnitudes of the drag vary from tens to hundreds of m s^{-1} sol^{-1} depending on the shape of simulated jets and assumed wave sources. "Orographic" GW schemes are now routinely used in some martian general circulation models (GCMs) (Forget et al., 1999; Hartogh et al., 2005). Subgrid-scale orographic GWs contribute up to ~10% of the Eliassen-Palm flux divergence due to resolved motions (Medvedev and Hartogh, 2007). Since the circulation in the martian MA is controlled by larger-scale eddies, mainly tides, it was thought that the former could be satisfactorily reproduced by GCMs without parameterized small-scale GWs.

Recently martian MA GCMs have been extended to thermospheric altitudes (González-Galindo et al., 2009), or specialized terrestrial thermosphere models have been adapted to Mars (Bougher et al., 2008). Given the lack of wind and temperature measurements in the upper atmosphere of Mars, most of our understanding of the dynamics at these heights comes from simulations. However, none of the GCMs use parameterizations for GWs with $c \neq 0$, or do not realistically account for propagation of GW spectra from the lower atmosphere and attenuation in the thermosphere. Thus, a significant part of the momentum and energy budget may be missing. Meanwhile, one-dimensional simulations of Parish et al. (2009) indicated that small-scale GWs can propagate into the martian thermosphere and generate appreciable body forcing. The resolved zonal GW torque was found to be comparable with the contributions of tides and planetary waves in the winter polar MA, at least during major dust storms (Kuroda et al., 2009).

This paper addresses the fundamental gap in knowledge of the momentum budget in the martian upper atmosphere. We quantify the GW momentum deposition of lower atmospheric origin at thermospheric heights by applying our recently developed spectral nonlinear GW parameterization (Yiğit et al., 2008, 2009) to wind and temperature distributions from the Mars Climate Database (MCD) that is based on the output of the Laboratoire de Météorologie Dynamique (LMD) GCM (González-Galindo et al., 2009).

2. Gravity wave scheme

Vertical propagation of GW harmonics in the thermosphere is affected by refraction due to the background wind and temperature, and by attenuation

* Corresponding author.
E-mail address: medvedev@mps.mpg.de (A.S. Medvedev).

0019-1035/$ - see front matter © 2010 Elsevier Inc. All rights reserved.
doi:10.1016/j.icarus.2010.10.013

associated with nonlinear effects (breaking and/or saturation) and dissipation (molecular and eddy diffusion, thermal conduction, ion friction, etc.). In the upper atmospheres of Mars and Earth, the molecular diffusion and heat conduction are the main damping mechanisms. Since the scheme is described in full detail by Yiğit et al. (2008), we provide only the relevant details.

The vertical momentum flux associated with an individual harmonic i in a GW spectrum, $F_i(z) \equiv \rho(z)\overline{u'w'}_i$, ρ being the mean density, u' and w' are fluctuations of horizontal and vertical velocities, correspondingly, varies with height, z, as

$$F_i(z) = F_i(z_0)\exp\left[-\int_{z_0}^{z}\left(\beta^i_{non}+\beta^i_{mol}\right)dz'\right], \quad (1)$$

where z_0 is the source height, and the vertical attenuation factors due to nonlinearity and molecular diffusion/conduction, β_{non} and β_{mol}, are (Medvedev and Klaassen, 1995, 2000; Yiğit et al., 2008):

$$\beta_{non} = \sqrt{2\pi}\frac{1}{\sigma_i}\exp\left(-\alpha_i^2\right), \quad \beta_{mol} = \frac{2\nu_{mol}N^3}{k_h(c_i-\bar{u})^4}. \quad (2)$$

In (2), the nonlinear damping that affects the given harmonic with the observed phase speed c_i is produced by all waves with smaller intrinsic phase velocities $(c_j-\bar{u}) < (c_i-\bar{u})$; $\sigma_i^2 = \Sigma_j \overline{u_j'^2}$ is the wind variance created by the waves with shorter vertical wavelengths, N is the Brunt–Väisälä frequency, $\alpha_i = \left(\sqrt{2}\sigma_i\right)^{-1}|c_i-\bar{u}|$, k_h is the horizontal wavenumber, ν_{mol} is the kinematic molecular viscosity. For a spectrum consisting of a single harmonic, β_{non} reduces to the Lindzen–Hodges saturation criterion but at ~70% $\left(1/\sqrt{2}\right)$ lower amplitudes. The total GW momentum flux is the sum of all individual components, and the total momentum deposition can be found as the divergence of this flux: $a = -\rho^{-1}dF/dz$.

Kinematic molecular viscosity ν_{mol} is related to the thermal conduction coefficient $k = AT^{0.69}$ via $k = 0.25[9c_p - 5(c_p - R)]\nu_{mol}$, c_p and R being the specific heat and gas constant, correspondingly, T is temperature. For the pure CO_2 atmosphere at martian conditions this yields the parameterization adopted in our calculations: $\nu_{mol} = 3.128T^{0.69}\times 10^{-7}/\rho$ ($m^2\,s^{-1}$). These distributions are in a good agreement with the profile presented by Parish et al. (2009, Fig. 2), and used in the work of González-Galindo et al. (2009).

Once the spectral distribution of wave momentum fluxes $F(z_0)$ is prescribed at a source height z_0, the vertical propagation of all GW harmonics and their associated momentum deposition can be calculated. The scheme does not require "intermittency coefficients" and other tunable parameters except for the characteristic horizontal wavenumber k_h.

3. Observational constraints on gravity waves

Creasey et al. (2006a) derived global and seasonal distributions of the wave activity in the lower atmosphere from MGS radio occultation data. They found that wave potential energy per unit mass, E_p, averaged between 10 and 30 km is typically up to few J kg^{-1} at mid- to high-latitudes. In low latitudes (~±20°) it increases up to 25 J kg^{-1}. For GWs with vertical wavelengths shorter than approximately a scale height, those we are most concerned with, Creasey et al. (2006a) find that E_p is about twice weaker. Note, that wave kinetic energy per unit mass, $E_k = \overline{u'^2}/2$, is approximately equal to E_p for mid- and high-frequency GW harmonics (e.g. Geller and Gong, 2010, Eqs. (7) and (8)). This gives the estimate for rms variations of horizontal wave velocity: $|u'| = \sqrt{2E_p}$.

Fritts et al. (2006) analyzed the ODY aerobraking data at high-latitude Northern Hemisphere winter to find typical GW velocity perturbations $|u'| \approx 70$ m s^{-1} and momentum fluxes $\overline{u'w'} \approx 2000$ $m^2\,s^{-2}$ at ~100 km or somewhat higher. Horizontal scales of wave fluctuations have been estimated between several tens and several hundreds km in both lower and upper atmospheres.

4. Results of simulations

Despite the lack of a "non-orographic" GW parameterization, the LMD GCM (González-Galindo et al., 2009) is the only model to date that self-consistently covers the atmosphere of Mars from the surface to the upper thermosphere. Temperature and especially wind crucially affect GW propagation, and we use the fields from the MCD as the background. Since the GW spectrum at the source level is not known, we employ the distribution that was observed in the Earth's troposphere, and is broadly used in GCMs (Yiğit et al., 2009 and the references therein):

$$\overline{u'w'} = \mathrm{sgn}(c_i-\bar{u}_0)\overline{u'w'}_{max}\exp\left[-(c_i-\bar{u}_0)^2/c_w^2\right], \quad (3)$$

where $\bar{u}_0$ is the mean wind at the source level and $c_w = 35$ m s^{-1}. In the calculations, the source height was taken just above typical convective cells at ≈250 Pa, or ~8 km. The spectrum was approximated with 30 harmonics $-60 \leqslant c - \bar{u}_0 \leqslant 60$ m s^{-1}. The only tunable parameter, the characteristic horizontal wavelength of the harmonics, was set to 200 km.

Fig. 1 shows the results of calculations for the MCD zonal mean wind and temperature averaged over the $L_s = 270$–$300°$ (winter in the Northern Hemisphere) season, and $\overline{u'w'}_{max} = 0.0025$ $m^2\,s^{-2}$. Note that the log-pressure altitudes have been calculated using the characteristic scale height $H = 9$ km. They are close to geometrical altitudes below ~110 km, but differ by 10–30 km in the upper thermosphere. Regions with absolute values of GW drag of more than 1000 m s^{-1} sol^{-1}, a magnitude expected from previous studies, are shaded. What immediately stands out is the huge drag created by GWs in the thermosphere. While in the Northern high-latitudes the drag is relatively in line with previous estimates, it exceeds 10^5 m s^{-1} sol^{-1} in the rest of the thermosphere. This unexpectedly strong GW momentum deposition is not an artefact of the poorly prescribed source spectrum, but a robust feature in our calculations. Fig. 1b shows that between 10 and 30 km σ is 1–2 m s^{-1}, which corresponds to $E_p = 0.5$–2 J kg^{-1}, and are at the lower end of the estimates of Creasey et al. (2006a). The momentum flux between 100 and 120 km is 500–3000 $m^2\,s^{-2}$ (Fig. 1c), close to the one inferred by Fritts et al. (2006). Results (not shown) of changing the source amplitude, its altitude, including or limiting faster harmonics alter the magnitude and height of the calculated GW drag maxima but do not appreciably change the overall behavior presented in Fig. 1.

The reason for the enormous GW effect in the thermosphere is in the assumed zonal wind distribution. The closure of the westerly jet in the winter hemisphere has been produced in the LMD GCM entirely by resolved tides and planetary waves without small-scale GWs. The strong easterly (retrograde) wind in the rest of the atmosphere is the consequence of the lack of eddy forcing. This wind filters out GW harmonics traveling in the same direction and favors the vertical propagation of others on their way to the thermosphere. For large $\bar{u}$, their intrinsic speed

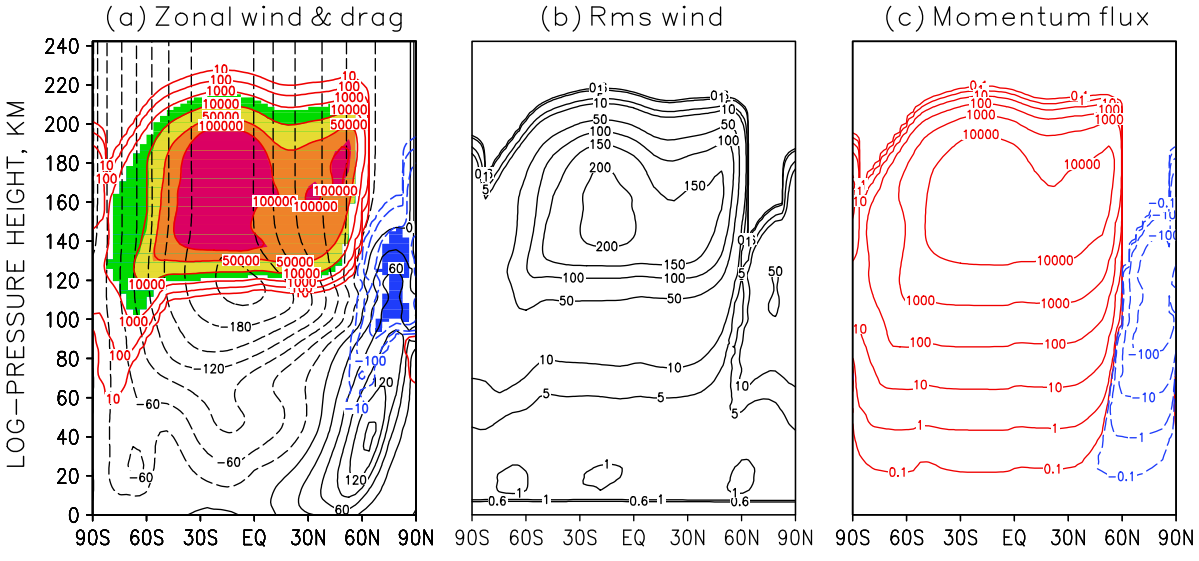

Fig. 1. (a) The background zonal wind at $L_s = 270$–$300°$ from the Mars Climate Database (black contour lines) and the calculated GW drag in (m s^{-1} sol^{-1}) (red and blue contour lines for eastward and westward directions, correspondingly). Color shadings highlight regions with GW drag exceeding |1000| m s^{-1} sol^{-1}, (b) rms horizontal wind fluctuations, σ, in (m s^{-1}), and (c) $\overline{u'w'}$ momentum flux in ($m^2\,s^{-2}$).

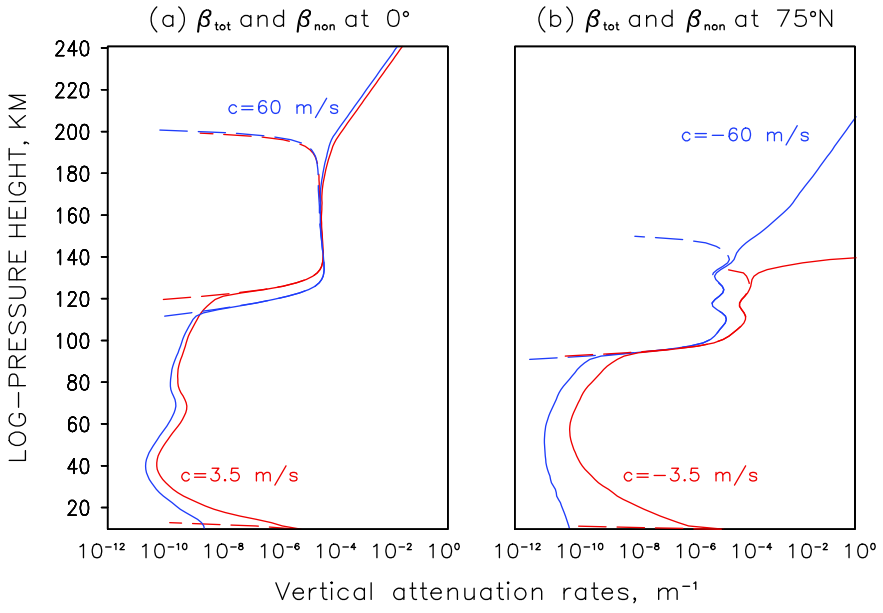

Fig. 2. Vertical damping coefficients: total (β_{tot}, solid lines) and due to nonlinearity (β_{non}, dashed lines) at the equator and 75°N. Red and blue lines correspond to the slower ($c = \pm 3.5$ m s^{-1}) and faster (± 60 m s^{-1}) harmonics, respectively, traveling against the mean wind.

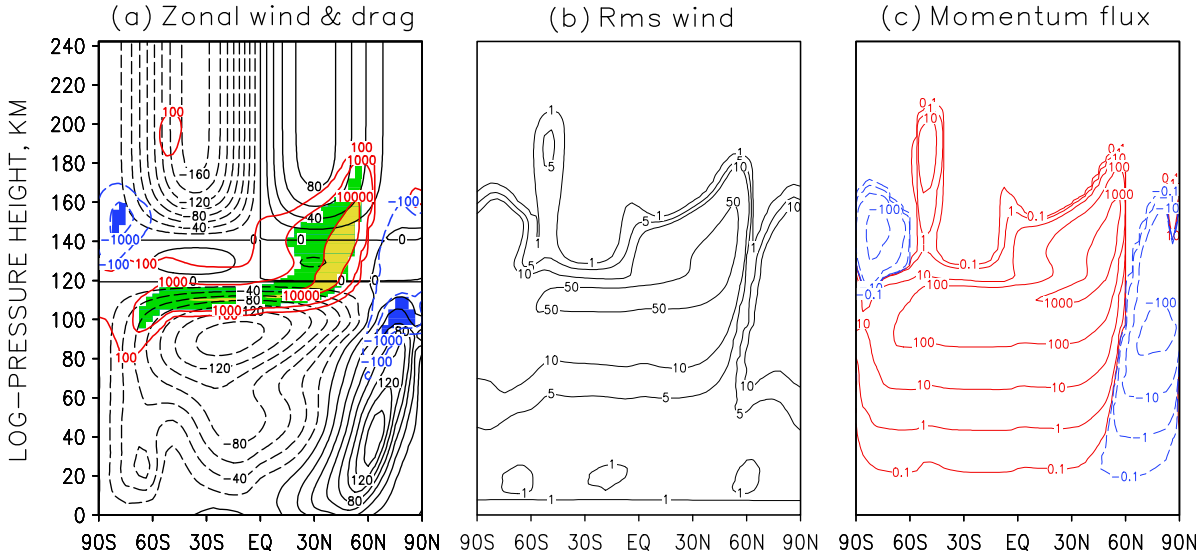

Fig. 3. Same as in Fig. 1 but for the case of modified background wind.

$|c_i - \bar{u}|$ becomes large as well, and following (2), the vertical damping by nonlinearity and molecular viscosity decreases. This mechanism is illustrated in Fig. 2 for the "fast" (60 m s^{-1}) and "slow" (3.5 m s^{-1}) waves traveling against the mean wind at the equator and at 75°N. Slower harmonics ($c = 3.5$) at the equator and $c = -3.5$ m s^{-1} in Northern high-latitudes are shown in red.[1] They are attenuated by the molecular viscosity stronger than the fast waves, but their amplitudes continue to grow with height. The onset of nonlinear damping occurs more abruptly when amplitudes are sufficiently large. The profiles of β_{non} are plotted with dashed lines of the corresponding color. At the equator, β_{non} dominates β_{mol} above 120 km, and produces most of its dissipation around 130–140 km. Unlike over the equator, at 75°N, the westerly wind decreases with height and changes sign. Therefore, $|c_i - \bar{u}|$ decreases, and β_{non} produces most of the damping at lower altitudes (90–120 km) where GW amplitudes are much weaker. In the upper thermosphere, the exponentially growing ν_{mol} eliminates the remaining harmonics. The momentum deposition by an individual dissipating harmonic is proportional to the product of β_{tot} and $\overline{u'w'}$. This explains why the GW drag is extremely large and located high in the thermosphere in our calculations.

Obviously, the calculated enormous wave drag is not compatible with the given zonal wind. If applied, it will rapidly weaken, and even reverse the easterly jet in the thermosphere. Interactive GCM simulations are required to reproduce the circulation with GWs accounted for. Here we only illustrate that changing background can decrease the GW drag and bring it closer with the previous estimates. A plausible assumption would be that $\bar{u}$ decreases and even changes sign somewhere below the maximum of the GW-induced torque. Additionally, the large westerly (prograde) momentum deposition would probably reverse the thermospheric easterlies in the winter hemisphere. Fig. 3 presents the results of calculations for the wind with such hypothetical reversals superimposed on the wind in Fig. 1. Harmonics saturate lower at smaller amplitudes, generating therefore weaker drag. The strong drag over ~30°N is apparently a consequence of the prescribed wind changes being overly simplistic, it will likely disappear in interactive simulations due to adjustments in the underlying wind. The total $\overline{u'w'}$ flux and the rms wind fluctuation between 100 and 120 km are somewhat smaller than in Fig. 1, but still close to the retrievals of Fritts et al. (2006).

5. Conclusions

Calculations with a recently developed spectral nonlinear GW scheme (Yiğit et al., 2008, 2009) and the wind and temperature from the Mars Climate Database

[1] For interpretation of color in Figs. 1–3, the reader is referred to the web version of this article.

(González-Galindo et al., 2009) reveal extremely strong GW drag in the martian thermosphere, which is incompatible with the zonal wind distribution. Our analysis shows that it is caused almost entirely by the easterly (retrograde) wind dominating the upper atmosphere. Being properly included in GCM simulations, GWs will likely alter the momentum budget and the circulation in the thermosphere, decrease and even reverse the mean zonal wind between 110 and 140 km, and introduce significant changes in the upper thermosphere. To date, there is no observational evidence for this conclusion because of the lack of systematic measurements above 100 km. Wind changes are accompanied by changes of temperature. It seems plausible that the layer at 110–130 km altitude measured with Mars Express SPICAM (Forget et al., 2009, which is systematically colder the one simulated with GCMs, is the result of GWs.

Acknowledgments

This work was partially supported by German Science Foundation (DFG) Grant HA 3261/4,5. We thank M. Hickey and the other anonymous reviewer for helpful comments.

References

Barnes, J.R., 1990. Possible effects of breaking gravity waves on the circulation of the middle atmosphere of Mars. J. Geophys. Res. 95, 1401–1421.

Bougher, S.W., Bielly, P.-L., Combi, M., Fox, J.L., Mueller-Wodarg, I., Ridley, A., Roble, R.G., 2008. Neutral upper atmosphere and ionosphere modeling. Space Sci. Rev. 139, 107–141. doi:10.1007/s11214-008-9401-9.

Collins, M., Lewis, S.R., Read, P.L., 1997. Gravity wave drag in a global circulation model of the martian atmosphere: Parameterization and validation. Adv. Space Res. 19 (8), 1245–1254.

Creasey, J.E., Forbes, J.M., Hinson, D.P., 2006a. Global and seasonal distribution of gravity wave activity in Mars' lower atmosphere derived from MGS radio occultation data. Geophys. Res. Lett. 33, L01803. doi:10.1029/2005GL024037.

Creasey, J.E., Forbes, J.M., Keating, G.M., 2006b. Density variability at scales typical of gravity waves observed in Mars' thermosphere by the MGS accelerometer. Geophys. Res. Lett. 33, L22814. doi:10.1029/2006GL027583.

Forget, F., Hourdin, F., Fournier, R., Hourdin, C., Talagrand, O., Collins, M., Lewis, S.R., Read, P.L., Huot, J.-P., 1999. Improved general circulation models of the martian atmosphere from the surface to above 80 km. J. Geophys. Res. 104, 24155–24175.

Forget, F., Montmessin, F., Bertaux, J.-L., González-Galindo, F., Lebonnois, S., Quémerais, E., Reberac, A., Dimarellis, E., López-Valverde, M.A., 2009. Density and temperatures of the upper martian atmosphere measured by stellar occultations with Mars Express SPICAM. J. Geophys. Res. 114, E01004. doi:1029:2008JE003086.

Fritts, D.C., Wang, L., Tolson, R.H., 2006. Mean and gravity wave structures and variability in the Mars upper atmosphere inferred from Mars Global Surveyor and Mars Odyssey aerobraking densities. J. Geophys. Res. 111, A12304. doi:10.1029/2006JA011897.

Geller, M.A., Gong, L., 2010. Gravity wave kinetic, potential, and vertical fluctuation energies as indicators of different frequency gravity waves. J. Geophys. Res. 115, D11111. doi:10.1029/2009JD012266.

González-Galindo, F., Forget, F., López-Valverde, M.A., Angelats i Colli, M., Millour, E., 2009. A ground-to-exosphere martian general circulation model: 1. Seasonal, diurnal, and solar cycle variation of thermospheric temperatures. J. Geophys. Res. 114, E04001. doi:10.1029/2008JE003246.

Hartogh, P., Medvedev, A.S., Kuroda, T., Saito, R., Villanueva, G., Feofilov, A.G., Kutepov, A.A., Berger, U., 2005. Description and climatology of a new general circulation model of the martian atmosphere. J. Geophys. Res. 110, E11008. doi:10.1029/2005JE002498.

Heavens, N.G., Richardson, M.I., Lawson, W.G., Lee, C., McCleese, D.J., Kass, D.M., Kleinboehl, A., Schofild, J.T., Abdou, W.A., Shirley, J.H., 2010. Convective instability in the martian middle atmosphere. Icarus 208, 574–589. doi:10.1016/j.icarus.2010.03.023.

Joshi, M.M., Lawrence, B.N., Lewis, S.R., 1995. Gravity wave drag in three-dimensional atmospheric models of Mars. J. Geophys. Res. 100, 21235–21245.

Kuroda, T., Medvedev, A.S., Hartogh, P., Takahashi, M., 2009. On forcing the winter polar warmings in the martian middle atmosphere during dust storms. J. Meteorol. Soc. Jpn. 87, 913–921. doi:10.2151/jmsj.87.913.

Medvedev, A.S., Hartogh, P., 2007. Winter polar warmings and the meridional transport on Mars simulated with a general circulation model. Icarus 186, 97–110.

Medvedev, A.S., Klaassen, G.P., 1995. Vertical evolution of gravity wave spectra and the parameterization of associated wave drag. J. Geophys. Res. 100, 25841–25853.

Medvedev, A.S., Klaassen, G.P., 2000. Parameterization of gravity wave momentum deposition based on a nonlinear theory of wave spectra. J. Atmos. Solar-Terr. Phys. 62, 1015–1033.

Parish, H.F., Schubert, G., Hickey, M.P., Walterscheid, R.L., 2009. Propagation of tropospheric gravity waves into the upper atmosphere of Mars. Icarus 203, 28–37. doi:10.1016/j.icarus.2009.04.031.

Théodore, B., Lellouch, E., Chassefiere, E., Hauchecorne, A., 1993. Solstitial temperature inversions in the martian middle atmosphere: Observational clues and 2-D modeling. Icarus 105, 512–528.

Yiğit, E., Aylward, A.D., Medvedev, A.S., 2008. Parameterization of the effects of vertically propagating gravity waves for thermosphere general circulation models: Sensitivity study. J. Geophys. Res. 113, D19106. doi:10.1029/2008JD010135.

Yiğit, E., Medvedev, A.S., Aylward, A.D., Hartogh, P., Harris, M.J., 2009. Modeling the effects of gravity wave momentum deposition on the general circulation above the turbopause. J. Geophys. Res. 114, D07101. doi:10.1029/2008JD011132.